International Journal of Geo-Information

MDPI

Article

Exploring Travel Mobility in Integrated Usage of Dockless Bike-Sharing and the Metro Based on Multisource Data

Hui Zhang [1,*], Yu Cui [1], Yanjun Liu [2], Jianmin Jia [1], Baiying Shi [1] and Xiaohua Yu [1]

[1] School of Transportation Engineering, Shandong Jianzhu University, Jinan 250101, China
[2] College of Transportation Engineering, Tongji University, 4800 Cao'an Road, Shanghai 201804, China
* Correspondence: zhanghui@sdjzu.edu.cn

Abstract: Dockless bike-sharing (DBS) is a green and flexible travel mode, which has been considered as an effective way to address the first-and-last mile problem. A two-level process is developed to identify the integrated DBS–metro trips. Then, DBS trip data, metro passenger data, socioeconomic data, and built environment data in Shanghai are used to analyze the spatiotemporal characteristics of integrated trips and the correlations between the integrated trips and the explanatory variables. Next, multicollinearity tests and autocorrelation tests are conducted to select the best explanatory variables. Finally, a geographically and temporally weighted regression (GTWR) model is adopted to examine the determinants of integrated trips over space and time. The results show that the integrated trips account for 16.8% of total DBS trips and that departure-transfer trips are greater than arrival-transfer trips. Moreover, the integrated trips are concentrated in the central area of the city. In terms of impact factors, it is found that GDP, government count, and restaurant count are negatively correlated with the number of integrated trips, while house price, entropy of land use, transfer accessibility index, and metro passenger flow show positive relationships. In addition, the results show that the GTWR model outperforms the OLS model and the GWR model.

Keywords: travel mobility; dockless bike-sharing; metro; integrated use; multisource data

check for updates

Citation: Zhang, H.; Cui, Y.; Liu, Y.; Jia, J.; Shi, B.; Yu, X. Exploring Travel Mobility in Integrated Usage of Dockless Bike-Sharing and the Metro Based on Multisource Data. *ISPRS Int. J. Geo-Inf.* **2024**, *13*, 108. https://doi.org/10.3390/ijgi13040108

Academic Editors: Wolfgang Kainz and Hartwig H. Hochmair

Received: 23 January 2024
Revised: 12 March 2024
Accepted: 22 March 2024
Published: 24 March 2024

Copyright: © 2024 by the authors. Licensee MDPI, Basel, Switzerland. This article is an open access article distributed under the terms and conditions of the Creative Commons Attribution (CC BY) license (https://creativecommons.org/licenses/by/4.0/).

1. Introduction

As a green travel mode, dockless bike-sharing (DBS) has become an essential part of sustainable transportation, which greatly enhances the accessibility of cities [1–3]. There are various advantages of DBS, such as convenient use, flexible stopping, low price, and no emission. Since 2016, the emerging DBS swept across the majority of cities in China. DBS could not only provide a user-friendly and flexible door-to-door service; it could also provide a seamless transfer service with public transport [4]. In many transit-oriented cities, DBS plays a key role in solving the first-and-last mile problems.

Public transport systems with priority policies are considered to be an effective way to alleviate urban diseases such as traffic congestion and air pollution [5]. The metro system is the main component of public transport, which provides fast, cleaner, and high-capacity service. However, the weak connections and low accessibility caused by low network density hinder the more widespread use of metro systems. The emerging DBS greatly promotes the use of metros and even alleviates road congestion [6]. In the past several years, there have been numerous studies on the connections between DBS and metro, focusing on the spatiotemporal characteristics [7,8], impact factors analysis [9–11], accessibility [12,13], network-based features [14,15], etc. Besides the metro, DBS could also connect with buses for first-and-last mile, which increases bus ridership [16,17].

The usage of DBS is affected by many factors, such as the built environment, weather, sociodemographic factors, and the pandemic [18–21]. Liu et al. pointed out that daily DBS trips were significantly related with the density, diversity, and most types of land-use, and the effect of density varies with hours [22]. Zhao and Li showed that distance is the

most crucial influence on transfer trips between metro and home or workplace [23]. A further study shows that 85% of DBS travel distances are within 2 km [14], and travelers prefer to choose busses for a longer travel time [24]. In China, commuters with school- or work-related trips are more likely to use DBS, while female, older, and low-income ones are less like to use it to connect metro [25]. In the USA, Mohiuddin et al. claimed that low-income users, people of color, and no-auto-owners were more likely than other groups to utilize bike-sharing for many purposes [20].

Detecting the transfer trips of DBS is a critical issue for studying the integrated use of DBS and the metro. Due to the different fare systems, it is difficult to achieve accurate transfer trips. A typical method to identify transfer trips is creating a distance buffer around each metro station. A study of Shanghai shows that 45% of check-in points are located within a 300 m radius of metro stations [26]. Ji et al. pointed out that 90% of transfer trips are finished within 300 m [25]. Lin et al. proposed 50 m as buffer distance, and Xing et al. suggested 100 m as the upper bound [27,28]. Yu et al. studied the spatiotemporal travel demand of DBS–metro with buffer distances from 30 m to 100 m [29]. Besides DBS, there are other travel modes that are used to transfer to the metro, such as walking, e-bikes, and busses. For longer distances, travelers prefer to use e-bikes and busses to connect with metro stations [30,31].

Understanding the travel patterns of integrated DBS and metro trips could promote the sustainable development of multimodal transportation. Previous studies undertook a lot of work to identify the spatiotemporal characteristics of the integrated use of DBS and the metro and the relationships between influence factors. However, there were limited studies focusing on the dynamic correlations between transfer trips and influence factors. In addition, most related studies did not consider the relationship between transfer trips and metro flow. As a significant transfer mode, the number of DBS transfer trips may be affected by metro flow. To fill these gaps, this study proposed a framework within which to explore the integrated usage of DBS and the metro considering metro flow and accessibility. The contributions are as follows:

(1) Propose a two-step recognition method for identifying more accurate transfer trips between dockless bike-sharing and the metro and divide the types of transfer trips into arrival-transfer trips and departure-transfer trips.
(2) Explore the spatiotemporal characteristics of arrival-transfer trips and departure-transfer trips and detect the accessibility and inequity of transfer trips.
(3) Adopt a geographically and temporally weighted regression (GTWR) model to better understand the mechanism of the impact of variables on transfer trips, considering factors such as the socioeconomic, land-use, and explanatory variables of the metro.

The rest of this paper is organized as follows. Section 2 gives the literature review. Section 3 presents the data descriptions. The identifications of transfer trips and methods are proposed in Section 4. Section 5 presents the results. Section 6 discusses the study. Finally, Section 7 concludes the paper.

2. Literature Review

2.1. Spatial-Temporal Characteristics of Bike-Sharing Trip

With the help of devices installed on DBS, the trip information of timestamps and locations can be recorded, which enables researchers to analyze the spatiotemporal characteristics. Previous studies did a lot of work on travel mobility, heterogeneity, and rebalance [28,32,33]. Li and Dai et al. argued that the rides peak hour was 18:00 and concentrated in the core area of cities [34]. Zheng et al. studied Mobike bike sharing system in Beijing and found that the unbalance of nodes in mobility OD network follows a power law distribution [35]. In recent years, network-based methods for DBS draw much attention. Yang et al. proposed graph-based approaches to study the changes in spatiotemporal travel behaviors of DBS when a new metro line came to operation, and they found the new metro service boosted nearby bike demand [36]. Tian et al. used complex network theory to study the dynamic evolution of demand fluctuation of bike-sharing by indicators of node strength,

average path length, and betweenness [37]. Zhang et al. proposed a spatial network analysis framework of DBS by dividing the studied area into grids, finding that the DBS network is assortative and positively autocorrelated with evident communities [38]. Recently, graph-based prediction of DBS short-term demand has become a hotspot [39–41]. Dasterdi and Morency proposed a CNN-LSTM deep learning method to predict DBS demand at community level, which outperforms other compared methods [42]. The COVID-19 pandemic brought many changes in traveler's behavior of bike-sharing, leading to trip decreases and a lower proportion of commuting trips [43]. Li et al. pointed out that the proportions of home, park, and grocery activities increased, while the proportions of leisure and shopping activities decreased during the lockdown period [44].

2.2. Impact Factors of DBS Use

There is a massive number of factors that impact the usage of DBS, such as weather, land-use, and sociodemographic factors. Li et al. studied the impact of weather and land use on DBS and found that rain, high humidity, and high temperatures are likely to reduce the use of DBS [45]. Moreover, they found the density of companies, residential buildings, and metro stations have a positive impact on DBS flows. Wu et al. proposed a geographically weighted regression (GWR) to test the impact of the built environment on bike-sharing and found that bike stations near public transit, restaurants, shopping malls, and educational and financial places have a high number of bike trips [46]. Transportation facilities, including bus and metro stops, are positively related to DBS usage [9,36]. Zhou et al. studied the integrated use of DBS and public transport (bus and the metro) and found that population density, number of workplaces, and number of shopping and eating places plays a key role in the integrated use of DBS and the bus system [47]. The outbreak of COVID-19 significantly impacted the use of DBS, which sharply reduced the use of DBS and changed the distributions of DBS [43,48]. There exists competition between DBS and buses [49], but COVID-19 weakened the competitive relationships between DBS and bus system [50]. Li et al. adopted OLS and GWR models to quantify the relationship between stop duration and explanatory variables, including three new features, namely, the proportion of overlapping area between the influence area of transit stations and the corresponding sub-region, and the average flow of subway stations [51]. Bi et al. studied the varying influences of the built environment on bike-sharing commuting and found that bike-sharing commute trips tend to be more consistent and frequent with the help of the metro service [52].

2.3. Integrated Use of DBS and the Metro

The accessibility of public transport is an important performance measure, which involves the ability of passengers to make use of public transport facilities [53]. Most studies of spatial accessibility emphasize physical access, like walking distance to a public transport station [54–57]. A local bus service is expected to attract passengers within 1/4 mile of a bus stop, while light rail can attract passengers within 1/2 mile [58]. The emerging DBS could significantly enhance the accessibility of public transport. Ma et al. pointed out that each unit increment of shared bikes significantly increases bus ridership by 0.54, 0.34, and 0.15 during a.m. peak, p.m. peak, and off-peak periods on the route level [59]. Li et al. studied the feeding modes to the metro, including walking, buses, private bikes, docked bike-sharing, e-bikes, cars, and taxi, and found that docked bike-sharing had the shortest average feeding time, about 8 min [60]. Chen et al. used online data to assess the role of DBS, and the results indicate that DBS systems play a positive role in assisting them to access activity [61].

The metro provides an effective way to travel for commuters and other people, but it cannot cover every corner of the city. The first-and-last mile problem has become a key obstacle for the expansive metro use. Traditional transfer modes for the metro include walking, bus, car, etc. [62–64]. DBS is recognized as an important transfer mode for the metro due to its convenient, cheap, and green travel. Travelers can rent and return it

anywhere via smart phone. Recently, the integrated use of DBS and the metro has become a hot research topic [8,12,29]. Shao et al. divided metro stations into seven types based on the characteristics of connection flow between bike-sharing and the metro [65]. Zhong et al. claimed that over 70% of DBS trips were intensively occurring in about 20% of the regions with community property [66]. Studies show that the built environment also has a crucial impact on the integrated use of DBS and the metro [9]. Identifying the integrated DBS trips is the critical issue to study the integrated use of DBS and the metro. However, it is difficult to explore the accurately integrated trips because DBS does not depend on smart cards. Researchers identify integrated trips according to the distance between metro stations and the origins and destinations of DBS [67,68].

3. Data Descriptions

The studied area is Shanghai, China. Shanghai is the economic and innovation center of China. The total area of Shanghai is 6340.5 square kilometers, with 16 districts. As of the end of 2022, the population of Shanghai was 24.76 million. Metro in Shanghai is one of the largest public systems in China with 20 lines and 508 stations in 2023. The DBS of Mobike was deployed in 2016. There were 13 bike-sharing companies with over 1.6 million bikes operating in Shanghai in August 2018. Figure 1 shows the study area of Shanghai and data source of the metro and DBS.

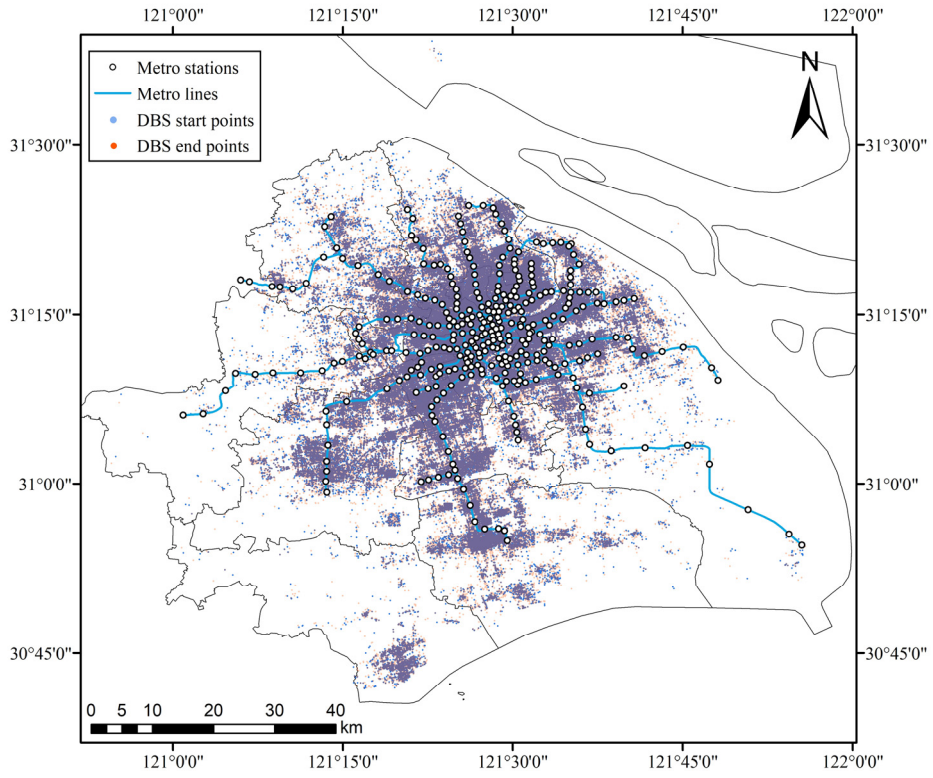


Figure 1. Study area of Shanghai and data source of metro and DBS.

The data used in this paper contain metro smart card data, DBS trip data, socioeconomic data (GDP, house price, and population density), and POI data, which are introduced as follows.

(1) DBS trip data. DBS trip data are also collected from 27 August 2018 to 2 September 2018. Table 1 shows the information of DBS trips, which contains the fields of "ID", "Start time", "Lon (O)", "Lat (O)", "End time", "Lon (D)", and "Lat (D)". The fields represent identification of DBS, start time of trip, longitude of trip origin, latitude of trip origin, end time of trip, longitude of trip destination, and latitude of destination, respectively.

(2) Metro smart card data. The metro smart card data are collected from 27 August 2018 to 2 September 2018. The fields of metro smart card data include "ID", "Date", "Time", "Line", "Station", and "Fare", which are shown in Table 2. Fare "0" means boarding; otherwise, it means alighting. We can extract the OD trips from the original smart card data.

(3) Socioeconomic data. The housing price data is from the Shanghai Anjuke Housing Price report [69]. GDP and population density data are from the Shanghai Urban Planning Bureau.

(4) POI data. In this paper, we apply a python program to obtain POI data from Baidu map (https://map.baidu.com/) (accessed on 1 August 2018). The POI data contain ten categories: "Hotel", "Government", "Business", "Science and education culture", 'Hospital', "Restaurant", "Shopping", "Public facilities", "Sports and leisure service", and "Scenic spot". It is noteworthy that the housing price data, GDP, population, POI, and road density are selected around metro stations with a 1300 m buffer.

(5) Road network data. The road network data used in this paper are collected from the OpenStreetMap (OSM) (https://www.openstreetmap.org/) (accessed on 1 August 2018). We mainly use road density in this paper. The road network data are also selected around metro stations with a 1300 m buffer.

Table 1. Information of DBS trip.

ID	Start Time	Lon (O)	Lat (O)	End Time	Lon (D)	Lat (D)
736E30	20180828170419	121.502	31.231	20180828172036	121.508	31.223
723F86	20180828135133	121.344	31.289	20180828141850	121.350	31.312
...	...	...	...	...	...	

Table 2. Information about metro smart card.

ID	Date	Time	Line	Station	Fare
7136	2018-8-28	07:36:33	6	Yuanshentiyuzhongxin	0
7136	2018-8-28	08:03:51	4	Linpinglu	3
...	...	...	...	...	...

The data should be cleaned before use. First, the starting point or ending point of trips outside the studied area will be removed. Second, trips with incomplete information, such as those lacking a timestamp or position, will be deleted. Finally, we calculate the Euclidean distance and travel time of each trip and remove the trips in which the distance is less than 200 m or greater than 10 km, as well as those in which the travel time is less than 2 min or more than 1 h [19]. After the data cleaning process, we obtained 5,616,151 DBS trips and 25,854,526 metro OD trips.

4. Methodology

4.1. Identification of Integrated DBS and Metro Trips

Identifying the integrated DBS and metro trips is the key issue in this study. Generally, integrated trips include two patterns: (1) cycling to a public transport station; and (2) cycling from a public transport station [47]. In this paper, we call the first pattern and second pattern arrival-transfer trips and departure-transfer trips, respectively.

Inspired by Liu et al. [68], we introduce a two-step identification method to explore the integrated trips between DBS and the metro. The first step is finding the DBS trips that fall into the metro station buffer at the spatial level. In this paper, we choose 100 m as the buffer radius around the metro stations. The second step is to match the integrated trips that were found in the first step with the corresponding metro operation time. The trips that were outside of operation time will be removed. As shown in Figure 2, if the starting point of a DBS trip is within any buffer zone of the metro station and the ending point does

not belong to any buffer zone, then the trip is departure-transfer trip; if the ending point of a DBS trip is within the buffer zone and the starting point does not belong to any buffer zone, then the trip is arrival-transfer trip. Specially, if the starting and ending points of DBS belong to different metro buffer zones, we choose that point with the shortest distance to metro stations to judge which transfer pattern it belongs to.

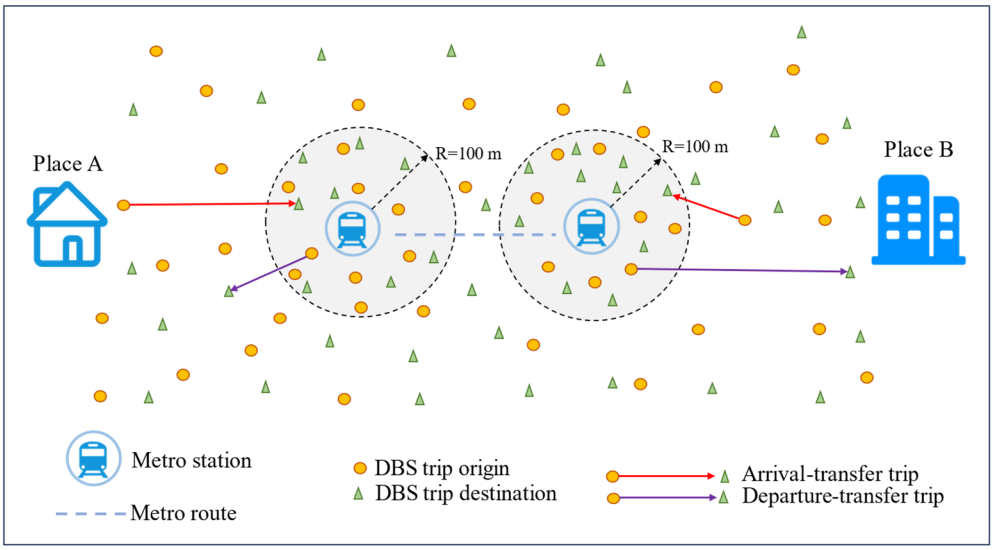


Figure 2. Illustration of identifying the integrated DBS and metro trips at the spatial level.

Based on the proposed two-step recognition method, 945,172 integrated trips have been identified, which accounts for 16.8% of total trips. Among them, there are 382,149 arrival-transfer trips, accounting for 40.4% of the total integrated trips, and there are 563,023 departure-transfer trips, accounting for 59.6% of the total integrated trips, as shown in Figure 3. The DBS departure-transfer trip is more than the DBS arrival-transfer trip, indicating that users prefer to use DBS to address the "last mile" problem. The reason is that users can find DBS easily around metro stations, where a large number of DBS are deployed.

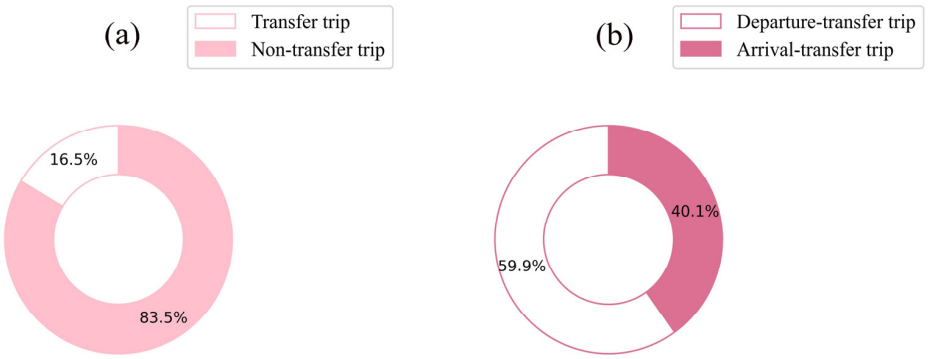


Figure 3. The proportions of (**a**) integrated trips and (**b**) arrival-transfer trip and departure-transfer trip.

To further detect the characteristics of transfer trips and non-transfer trips, we plot the distributions of (a) distance and (b) time for transfer trips and non-transfer trips in Figure 4. We can see that the most integrated trips' distances are concentrated between 0 km and 2 km. The travel time of integrated trips are concentrated between 0 min and 30 min. The travel times of DBS trips are affected by the road congestion. Therefore, the travel time distribution of integrated trips spans widely compared to the travel distance.

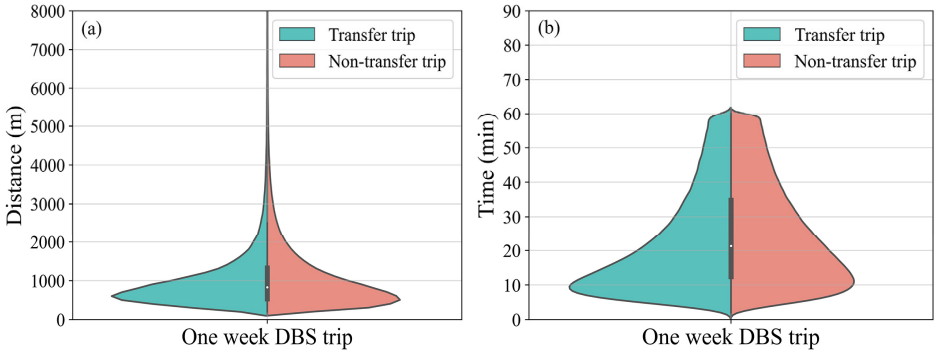


Figure 4. Distributions of (**a**) distance and (**b**) time for transfer trips and non-transfer trips.

4.2. Independent Variables

There are many factors that affect the number of integrated trips, including socioeconomic, land-use, and transportation factors [70]. As shown in Table 3, we adopt socioeconomic, land use, and metro-related factors as independent variables. Because most integrated trips are shorter than 1300 m, we set 1300 m as the buffer radius around metro stations to calculate the values of the independent variables.

Table 3. Definition and description of variables.

Variables	Description	Mean	Std.
Dependent variables			
DBS for arrival-transfer trips (weekday)	Hourly number of arrival-transfer trips of each metro station on weekdays	47.01	44.73
DBS for departure-transfer trips (weekday)	Hourly number of departure-transfer trips of each metro station on weekdays	69.85	66.80
DBS for arrival-transfer trips (weekend)	Hourly number of arrival-transfer trips of each metro station on weekends	11.77	10.26
DBS for departure-transfer trips (weekend)	Hourly number of departure-transfer trips of each metro station on weekends	16.14	14.16
Explanatory variables			
Socioeconomic			
GDP	GDP at 1300 m buffer zone (billion)	4186.84	3827.26
House price	Average housing price at 1300 m buffer zone (yuan/m^2)	55,527.46	17,704.27
Population density	Population divided by area in the 1300 m buffer zone (people/km^2)	8375.19	9947.02
Land use			
Hotel count	Number of hotel pois in the 1300 m buffer zone	90.39	110.07
Government count	Number of governmental pois in the 1300 m buffer zone	63.33	77.96
Business count	Number of commercial pois in the 1300 m buffer zone	296.21	383.68
Science and education culture count	Number of cultural pois in the 1300 m buffer zone	93.16	138.89
Hospital count	Number of hospital pois in the 1300 m buffer zone	35.09	44.95
Bus stop count	Number of bus stop pois in the 1300 m buffer zone	81.83	61.78
Restaurant count	Number of restaurant pois in the 1300 m buffer zone	157.58	166.32
Shopping mall count	Number of shopping mall pois in the 1300 m buffer zone	13.07	11.12
Road density	Length divided by area in the 1300 m buffer zone (km/km^2)	4.61	3.10
Entropy of land use	The degree of mixture of land use in the 1300 m buffer zone	0.73	0.13
Metro			
Number of metro stations	Number of metro stations in the 1300 m buffer zone	2.77	1.65
Passenger flow of each metro station	Hourly inbound passenger flow on weekdays	3269.47	3988.87
	Hourly outbound passenger flow on weekdays	3220.29	3996.45
	Hourly inbound passenger flow on weekends	1016.38	1346.12
	Hourly outbound passenger flow on weekends	937.02	1315.76
Transfer accessibility index at each metro stations (min)	Hourly of arrival-transfer trips of time on weekday	0.06	0.02
	Hourly of departure-transfer trips of time on weekday	0.06	0.02
	Hourly of arrival-transfer trips of time on weekend	0.05	0.02
	Hourly of departure-transfer trips of time on weekend	0.06	0.02

Socioeconomic factors, such as population and income, are considered crucial factors that impact the ridership of public transport [71,72]. In this paper, we adopt three kinds of socioeconomic factors, including GDP, population, and house price. Land use is another very essential impact factor. Typically, the travel activities and behaviors of travelers in different kinds of land use types are different. To measure the differences of different land use mixes, the entropy of land use is introduced, which is calculated as follows [66].

$$E_i = -\frac{\sum_j p_j \ln(p_j)}{\ln(k)}, \quad (1)$$

where p_j is the proportion of one land use type in the buffer area of station i, and k is the number of land use types.

In this study, we choose three kinds of metro-related factors as independent variables, including the number of metro stations within the buffer zone, the passenger flow of the metro station, and the transfer accessibility index. The passenger flow of the metro includes both inbound passenger flow and outbound passenger flow. Accessibility is an important indicator to measure the station usefulness and convenience [4,38]. In this paper, we introduce a transfer accessibility index to measure the accessibility of the metro station, considering the travel time of integrated trips as follows:

$$A_i = \frac{1}{n_i} \sum_{j=1}^{n_i} \frac{1}{t_{ij}}, \tag{2}$$

where t_{ij} is the travel time from integrated DBS origin to destinations of trip j for metro station i, and n_i is the total number of integrated DBS trips within the buffer area of metro station i.

4.3. Variables and Regression Models

This paper utilizes the OLS model, GWR model, and GTWR model to explore the relationship between the number of integrated trips and explanatory variables. Before the models are applied, the multicollinearity test should be conducted because if there exists multicollinearity in independent variables, the regression models will result in unstable and unreasonable regression coefficient [7]. We selected explanatory variables with VIF value less than 10 and p-values less than 0.05. Similarly, the spatial autocorrelation of variables should be tested before using spatial regression models, and the explanatory variables with p-value less than 0.05 are selected.

4.3.1. Ordinary Least Square Regression (OLS)

The OLS model is a basic model used to find the relationship between a dependent variable and a range of independent variables. It is noteworthy that the OLS model neglects the spatial variations. In this paper, the model can be expressed as follows [47,73]:

$$y_i = \beta_0 + \sum_{j=1}^{m} \beta_j x_{ij} + \varepsilon_i, \tag{3}$$

where y_i is the dependent variable, x_{ij} is the jth independent variable, m is the number of independent variables, β_0 is the estimated intercept, β_{ij} is the regression coefficient of the jth independent variable, and ε_i is the random error term.

4.3.2. Geographically Weighted Regression (GWR)

In order to better deal with the spatial data regression, a GWR model is designed that allows for coefficients to vary across space. It can be seen as the extension of OLS model by associating explanatory variables with geographical locations, which can be expressed as follows [74]:

$$Y_i = \beta_0(u_i, v_i) + \sum_k \beta_k(u_i, v_i) X_{ik} + \varepsilon_i, \tag{4}$$

where $i (i = 1, 2, \cdots, n)$ is a TAZ, which is a most common regionalism in transportation studies; Y_i is the integrated trips volume in TAZ i; (u_i, v_i) are the coordinates of TAZ i; $\beta_0(u_i, v_i)$ is the intercept; X_{ik} is the kth explanatory variable; and $\beta_k(u_i, v_i)$ is the regression coefficient between integrated trips volume and the explanatory variables. The distinct characteristic of the GWR model is that the coefficient $\beta_k(u_i, v_i)$ varies across the model to measure the spatial variations of observations compared with the OLS model in which the parameter estimation is fixed for each observation.

4.3.3. Geographically and Temporally Weighted Regression (GTWR)

In many transportation systems, the number of travelers fluctuates and shows an obvious tidal property. The GWR model cannot deal with the temporal nonstationarity, which is a very important impact factor. Huang et al. introduced the GTWR model, which considers spatial and temporal variation simultaneously to extend the GWR model [75]. The GTWR model can be defined as follows:

$$Y_i = \beta_0(u_i, v_i, t_i) + \sum_k \beta_k(u_i, v_i, t_i) X_{ik} + \varepsilon_i, \quad (5)$$

where Y_i is the hourly integrated trip volume; X_{ik} is the kth explanatory variable, including hourly metro inbound passenger volume, hourly metro outbound passenger volume, socioeconomic, and land use variables; u_i, v_i, and t_i are the longitude, latitude, and time of TAZ i, respectively. $\beta_0(u_i, v_i, t_i)$ is the intercept value; and $\beta_k(u_i, v_i, t_i)$ is a range of parameter values in TAZ i. The regression coefficients of GTWR are estimated based on local weighted least squares, which can be expressed by the formula as follows [74,76]:

$$\hat{\beta}(u_i, v_i, t_i) = \left[X^T W(u_i, v_i, t_i) X\right]^{-1} X^T W(u_i, v_i, t_i) Y, \quad (6)$$

where the space–time weight matrix $W(u_i, v_i, t_i)$ depends on the space–time distance. The space–time weight can be calculated after defining the space–time distance. The commonly used weighting function is the decay-based Gaussian distance, which is expressed as follows [76]:

$$W_{ij} = \exp\left[-\frac{(d_{ij}^{ST})^2}{h^2}\right]. \quad (7)$$

Here, d_{ij}^{ST} is the space–time distance between TAZ i and j, which can be achieved by the formula as follows:

$$d_{ij}^{ST} = \sqrt{\lambda[(u_i - u_j)^2 - (v_i - v_j)^2] + \mu(t_i - t_j)^2}. \quad (8)$$

λ and μ are the weights for balancing different effects because space distance and time are measured by different units.

h in Equation (7) is a positive parameter called the space–time bandwidth, and the optimal bandwidth is achieved based on the minimum cross-validation (CV) value. The CV value is the sum of the squared error between the real value y_i and the predicted value $\hat{y}_i(h)$:

$$CV(h) = \sum_i (y_i - \hat{y}_i(h))^2. \quad (9)$$

The corrected Akaike information criterion (AIC) is an effective way to select the bandwidth [75]. We can use a GTWR plugin of ArcGIS to construct OLS, GWR, and GTWR models in this study [77].

5. Results

5.1. Spatiotemporal Characteristics of Integrated Trips

5.1.1. Temporal Characteristics of Integrated Trips

In order to detect the temporal characteristics of integrated trips, we plot the distributions of the number of metro trips, total DBS trips, arrival-transfer trips, and departure-transfer trips in Figure 5. It can be observed that the four kinds of trips have two peak hours in the morning (7:00–9:00) and evening (17:00–19:00), which show obvious commuting characteristics. This result is in line with the previous studies [69]. Moreover, there is a slight peak around 12:00 for integrated trips, which may be because some workers travel for activities at lunch time. On weekends, the number of travelers decreases sharply and shows no obvious peaks for the metro. However, there is one or two peaks for DBS trips

on weekends. The distributions of integrated trips, including arrival-transfer trips and departure-transfer trips, are very similar to total DBS trips distribution. However, the start time of integrated trips are different because the integrated trips depend on the operation time of the metro.

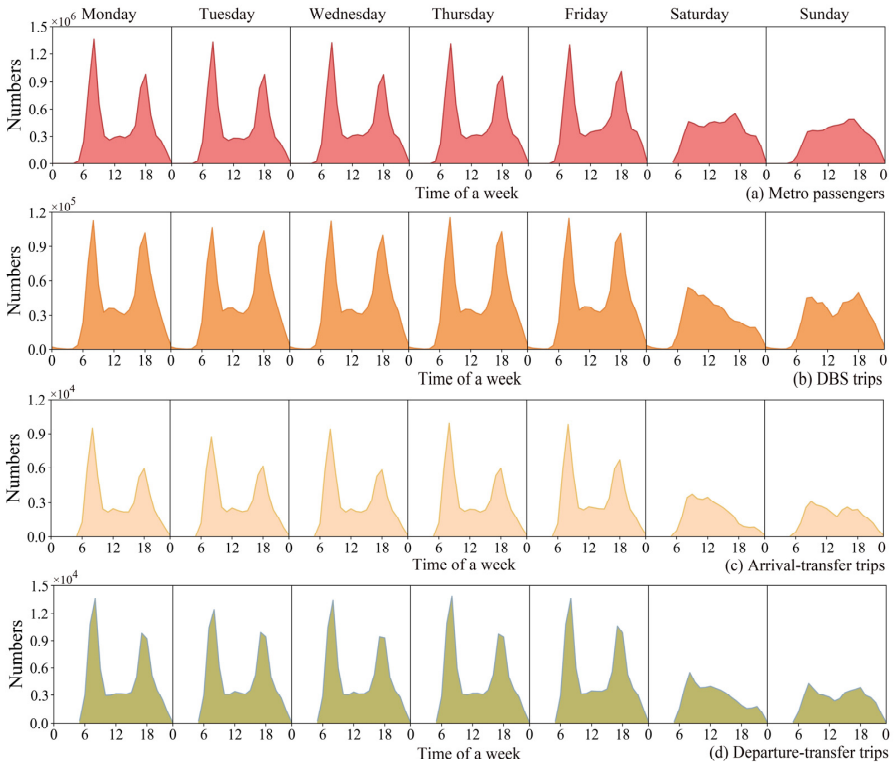


Figure 5. Distributions of the number of travelers in a week: (**a**) metro trips; (**b**) DBS trips; (**c**) arrival-transfer trips; (**d**) departure-transfer trips.

5.1.2. Spatial Characteristics of Integrated Trips

Figure 6 shows the spatial distributions of integrated trips on weekdays and weekends. The results show that the integrated trips, including arrival-transfer trips and departure-transfer trips, are concentrated in the central area. There are almost no integrated trips in the suburb far away from center area, such as to some stations of Line 16. The reason is that the DBS company did not deploy DBS in the area due to the high operation and management cost.

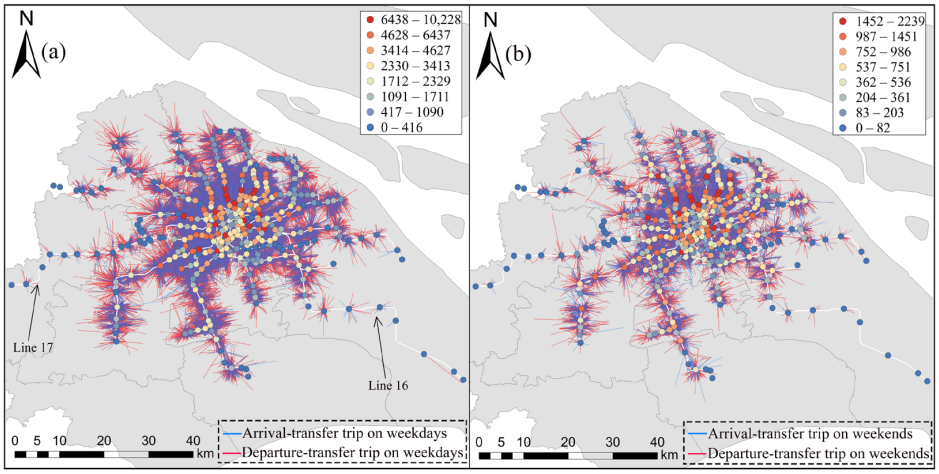


Figure 6. Spatial distributions of integrated trips of DBS–metro on (**a**) weekdays and (**b**) weekends.

5.1.3. Distributions of Integrated Trip Distance and Travel Time

Figure 7 shows the distributions of travel distance and time for arrival-transfer trips and departure-transfer trips. The distance of the DBS trips is calculated by the coordinates of origins and destinations. The travel time is calculated by subtracting the trip start time from the trip end time. As shown in the figure, both trip distance and travel time follow lognormal distributions. The median values of travel distance of arrival-transfer trips and departure-transfer trips are 770.9 m and 832.4 m, respectively. The median value of travel distance for departure-transfer trips is larger than that of arrival-transfer trips. The reason is that DBS is easier to be found around the metro stations, which attracts more passengers who travel longer distances and live in the suburbs. In contrast, it is found that the median value of the travel time of departure-transfer trips is smaller than that of arrival-transfer trips. Specifically, the median values of departure-transfer trips and arrival-transfer trips are 17 min and 20 min, respectively. The reason may be that the morning road congestion in Shanghai is more serious, and commuters have to spend more time cycling to metro stations.

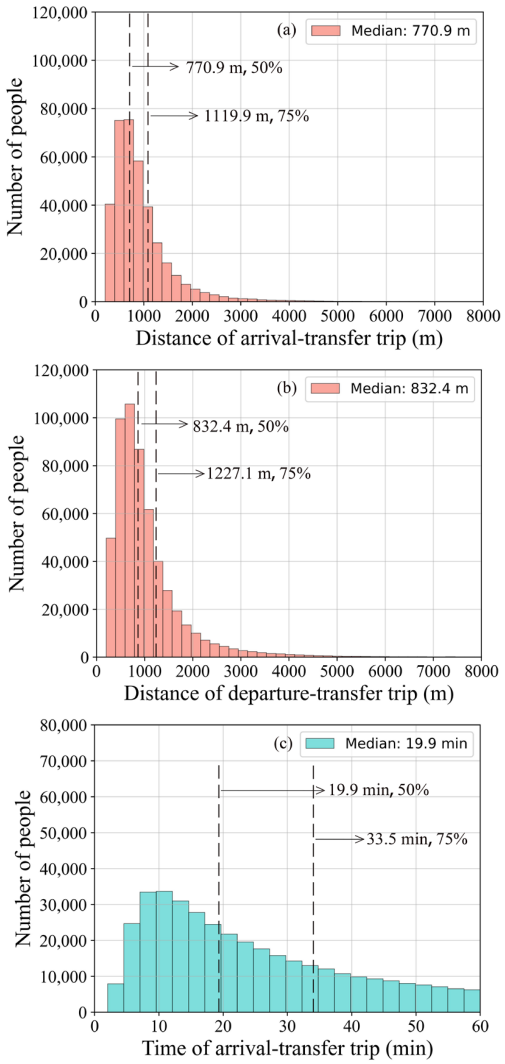


Figure 7. *Cont.*

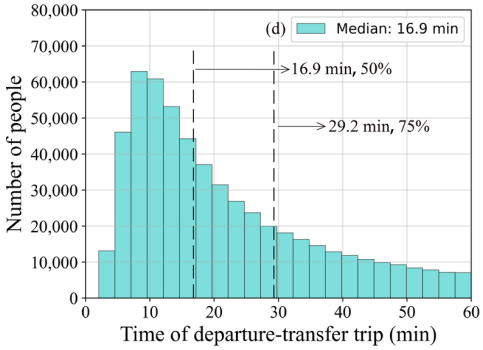


Figure 7. Distributions of (**a**) travel distance of arrival-transfer trip, (**b**) travel distance of departure-transfer trips, (**c**) travel time of arrival-transfer trip and (**d**) travel time of departure-transfer trips.

5.2. Spatial Distribution of Transfer Accessibility Index of Integrated Trips

Figure 8 shows the spatial distributions of the transfer accessibility index of integrated trips, including arrival-transfer trips and departure-transfer trips, within the buffer zone of each metro on weekdays and weekends. The larger value means travelers could spend less time connecting to metro stations via DBS. As can be seen in the figure, the transfer accessibility in the central area is higher than that in the suburbs, which indicates that travelers can spend less time transferring from/to the metro. In the suburbs, travelers may spend more time due to the low-density DBS distribution. Moreover, we can observe that the transfer accessibility index values of both arrival-transfer trips and departure-transfer trips are larger on weekdays than on weekends. The reason is that travelers can travel longer to connect to the metro without the limitations of time on the weekends. Another reason is that there is a large number of people that are closer to metro stations who travel for commuting. In addition, we can see that the transfer accessibility index values of departure-transfer trips are larger than those of arrival-transfer trips in the central area on both weekdays and weekends. The results imply that travelers prefer to use bike-sharing after they use the metro.

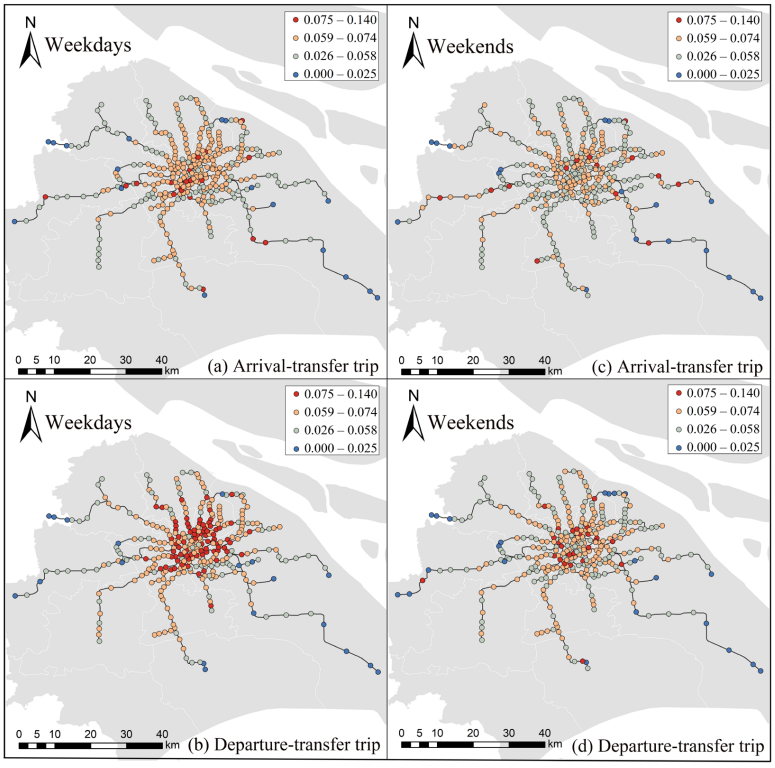


Figure 8. Spatial distribution of transfer accessibility index of integrated trips.

5.3. Spatial Distributions of Entropy of Land Use

As shown in Figure 9, we draw the spatial distributions and value distributions of the entropy of land use within the buffer zones. It is observed in Figure 9a that the buffer zones around most metro stations in the central area have high values of entropy of land use, which means there is even distribution of land types. There exist some buffer zones of metro stations in suburbs with low values. But the proportion of these stations is small. Some buffer zones of metro stations in suburbs also have high values. The reason is that the facilities around the metro stations are better than those in other areas due to the transportation convenience. In total, we can see in Figure 9b that most values of entropy of land use are concentrated between 0.5 and 0.9, and the median value is 0.782. The results indicate that the facilities around most metro stations are evenly distributed.

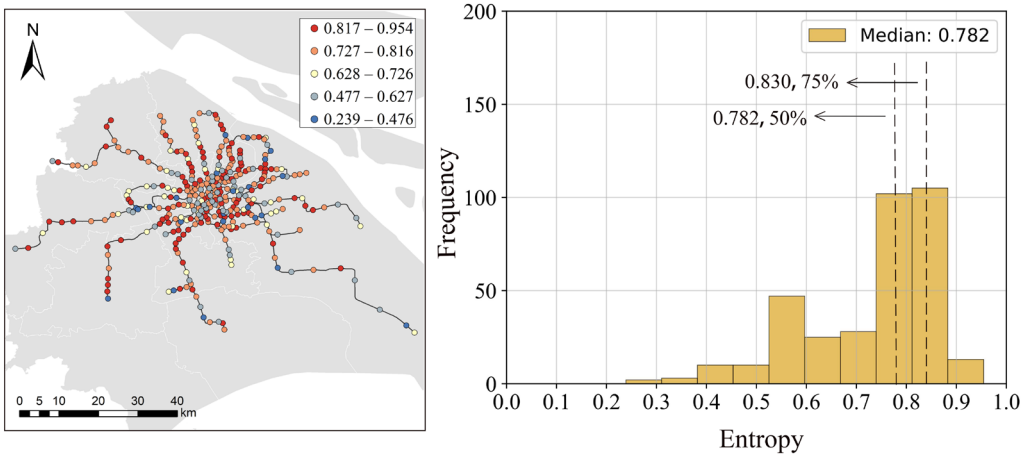


Figure 9. Statistical results of the entropy of land use: (**a**) spatial distributions, (**b**) value distributions.

5.4. Regression Model Results

5.4.1. Model Comparison

In this paper, we used the OLS model, the GWR model, and the GTWR model to test the arrival-transfer trips and departure-transfer trips on weekdays and weekends, respectively. We calculates the VIF index of all independent variables, and the variables with VIF larger than 10 and p-values larger than 0.05 were removed from the regression. Then, OLS models were used to test the significance of the selected explanatory variables for both arrival-transfer trips and departure-transfer trips. The selected explanatory variables and the results of OLS regression are shown in Tables A1 and A2, respectively. The results show that the selected explanatory variables for arrival-transfer trips and departure-transfer trips are different. For example, the POI of business count is not selected for arrival-transfer trips on weekdays because the VIF value is larger than 10 and the p-values are larger than 0.05, but it is selected for departure-transfer trips on weekdays. It is found that GDP, government count, and restaurant count are negatively correlated with the number of arrival-transfer trips and departure-transfer trips. In addition, we found house price, entropy of land use, transfer accessibility index, and metro passenger flow to be positively related to the numbers of two transfer trips.

The Moran's I was applied by ArcGIS 10.3 to test whether the variables are spatially autocorrelated. Table A3 shows the main results, including Moran's I, Z-score, and p-value. We selected the variables with a p-value that is smaller than 0.05 to conduct the GWR and GTWR models. These two models will create an output feature class and a statistical summary report of the model. R^2 and AICc are two indicators widely used to assess the performance of the models. Table 4 exhibits the performances of the OLS model, the GWR model, and the GTWR model. The results indicate that the GTWR model outperforms the other two models because it is the model with larger R^2 and smaller AICc values. Taking

arrival-transfer trips as an example, the R^2 values are 0.43, 0.57, and 0.81 for the OLS model, GWR model, and GTWR model, respectively.

Table 4. Performances of the OLS model, GWR model, and GTWR model.

	Arrival-Transfer Trip				**Departure-Transfer Trip**			
	Weekday		Weekend		Weekday		Weekend	
	AICc	R^2	AICc	R^2	AICc	R^2	AICc	R^2
OLS	−336.16	0.43	−313.00	0.44	−291.17	0.47	−259.23	0.44
GWR	−353.96	0.57	−348.79	0.59	−312.36	0.59	−264.04	0.52
GTWR	−16,188.00	0.81	−10,647.90	0.78	−14,092.20	0.80	−8203.31	0.76

5.4.2. Temporal Features of Variable Coefficient

Compared with the GWR model, we can achieve the time series of the hourly coefficient from the GTWR model. Tables 5 and 6 show the estimation of the GTWR model for arrival-transfer trips and departure-transfer trips, respectively. As an example, we discuss the fluctuation of the average coefficient of metro passenger flow, the entropy land use, the transfer accessibility index, and the GDP over time in a day in Figure 10. The positive coefficient means there is a positive relationship between the dependent and explanatory variables and vice versa.

Table 5. Estimation of the GTWR model for arrival-transfer trip.

	Min	**Max**	**Avg**
Weekday			
Explanatory variables of socioeconomic			
GDP	−7.110	5.197	−0.037
House price	−1.748	3.115	0.079
Explanatory variables of land use			
Hotel count	−1.321	2.904	0.113
Government count	−1.751	2.898	−0.064
Hospital count	−2.419	2.044	0.042
Restaurant count	−2.321	0.788	−0.071
Entropy of land use	−0.786	0.822	0.006
Explanatory variables of metro			
Number of metro station	−1.008	0.721	−0.003
Hourly inbound passenger flow	−1.218	4.959	0.508
Transfer accessibility index	−1.622	4.741	0.332
Weekend			
Explanatory variables of socioeconomic			
GDP	−9.780	8.878	−0.162
House price	−1.494	3.400	0.075
Explanatory variables of land use			
Hotel count	−10.686	13.704	0.058
Government count	−3.067	5.560	−0.158
Science and education culture count	−4.377	21.178	0.482
Hospital count	−10.405	3.480	0.101
Restaurant count	−5.542	2.402	−0.154
Entropy of land use	−0.677	1.385	0.031
Explanatory variables of metro			
Number of metro station	−5.518	1.775	0.018
Hourly inbound passenger flow	−4.301	7.037	0.621
Transfer accessibility index	−1.096	3.279	0.174

Table 6. Estimation of the GTWR model for departure-transfer trip.

	Min	Max	Avg
Weekday			
Explanatory variables of socioeconomic			
GDP	−6.211	6.328	0.010
House price	−2.158	2.753	0.057
Explanatory variables of land use			
Hotel count	−4.331	9.541	0.129
Government count	−2.496	2.851	−0.068
Business count	−4.055	4.539	0.047
Hospital count	−2.782	2.511	0.029
Restaurant count	−2.323	2.339	−0.091
Entropy of land use	−0.973	1.010	0.013
Explanatory variables of metro			
Hourly outbound passenger flow	−2.308	15.427	0.954
Transfer accessibility index	−1.403	2.044	0.211
Weekend			
Explanatory variables of socioeconomic			
GDP	−15.224	10.137	−0.168
House price	−1.841	3.891	0.173
Explanatory variables of land use			
Hotel count	−5.761	15.546	0.198
Government count	−5.703	5.738	−0.117
Hospital count	−9.590	7.862	0.137
Restaurant count	−6.214	2.982	−0.166
Entropy of land use	−1.282	2.057	0.024
Explanatory variables of metro			
Hourly outbound passenger flow	−4.658	23.937	0.870
Transfer accessibility index	−1.905	7.181	0.599

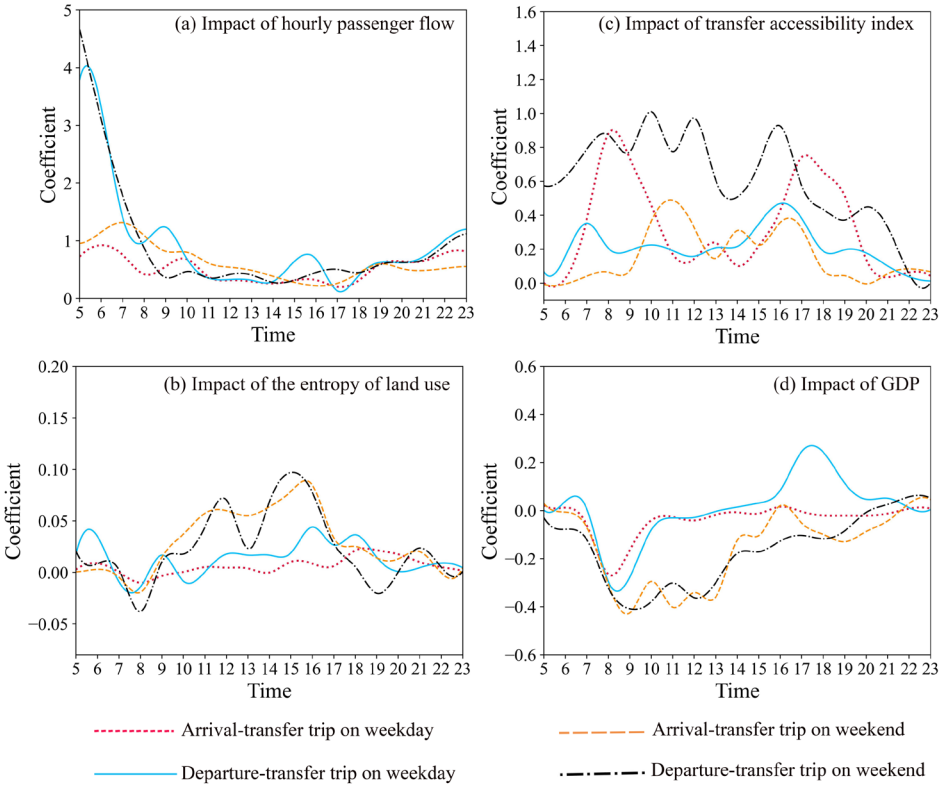


Figure 10. Temporal distribution of the average coefficients of hourly passenger flow, entropy of land use, transfer accessibility index, and GDP.

From Figure 10a, we can see that there is a positive relationship between transfer trips and metro passenger flow. Specifically, it shows that the positive effect of metro passenger flow on arrival-transfer trips in off-peak hours is stronger than that in peak hours on weekdays. This can be explained by the fact that passengers dislike to use bike-sharing to connect to the metro in peak hours due to the low speed of bikes and bad road conditions in some areas. The positive effect of metro passenger flow on departure-transfer trips before morning peak hours is stronger than that in other time periods on weekdays, and the reason may be that it is easier to find a bike before morning peak hours.

Figure 10b shows that there is a positive relationship between the entropy of land use and transfer trips. From Figure 10b, it can be observed that the positive effect of the entropy of land use on transfer trips is more pronounced during commuting time, for example, departure-transfer trips around 6:00 and 17:00 on weekdays. The impact of the entropy of land use on arrival-transfer trips and departure-transfer trips during the weekend is mainly reflected in the noon period, which may be related to residents' entertainment travel activities, which involve various activities such as shopping, dining, sports and leisure activities, and sightseeing activities.

From Figure 10c, we can see that the transfer accessibility index has a positive impact on transfer trips. It can be found that the peak value of the impact is consistent with the peak commuting time on weekdays. Moreover, the impact on arrival-transfer trips on weekdays is particularly significant, indicating that a good transfer accessibility index promotes commuting activities for residents. The peak value of the impact is consistent with the entertainment travel time of residents on weekends, which also reflects the good transfer accessibility index, providing convenience for residents' entertainment travel.

Figure 10d shows the relationship between GDP and transfer trips. It indicates that the impact of GDP on transfer trips is generally negative. DBS travel is a green, convenient, and low-cost mode of transportation, and the impact of economic development on transfer travel is not significant. According to Figure 10d, we can also determine that the negative impact of GDP on arrival-transfer trips and departure-transfer trips is most significant during the morning peak on weekdays, while the impact is not significant during other time periods. The impact of GDP on arrival-transfer trips and departure-transfer trips on weekends is similar to that on weekdays. However, the impact on weekends fluctuates more, possibly due to the different travel purposes of residents on weekdays and weekends.

5.4.3. Spatial Feature of Variable Coefficient

The spatial distributions of the average coefficients of hourly passenger flow are shown in Figure 11. The effects of hourly passenger flow on both arrival-transfer trips and departure-transfer trips in the central area are small, and even some stations' passenger flow has a negative impact on the number of integrated trips within the buffers. However, there are positive effects in the suburbs for arrival-transfer trips and departure-transfer trips. In the periphery of the city, the positive effects are even stronger. The reason is that the traffic facilities in the central area of the city are much better than those in the suburbs, in which travelers can choose other travel modes to connect to metro stations [9]. In the suburbs, the traffic facilities (e.g., bus stations) are sparsely distributed, and travelers prefer to use bike-sharing to connect to metro stations. Moreover, it can be seen that the effects on departure-transfer trips are stronger than those of arrival-transfer trips on weekdays and weekends. The reasons may be that it is easier to find a bike-share near the metro station than the home or workplace and that people like to use bike-sharing when they exit the metro stations.

Figure A1 shows the spatial distributions of the average coefficients of the entropy of land use. We can see that the impact coefficient of the entropy land use on transfer trips shows a wide and extensive positive distribution. Figure A1a and Figure A1b, respectively, show the impact of the entropy of land use on arrival-transfer trips and departure-transfer trips on weekdays. It can be seen that there is a negative impact of the entropy of land use on transfer trips in some central areas. The reason may be that residents can choose

other modes of transportation to reach their destinations in the areas with developed transportation, complete infrastructure, and diverse activity scenarios. In some suburban areas, there are a few sites with negative impacts, which may be due to inadequate land use in the area. In addition, it is worth noting that the entropy of land use on weekends has a strong impact on arrival-transfer trips and departure-transfer trips.

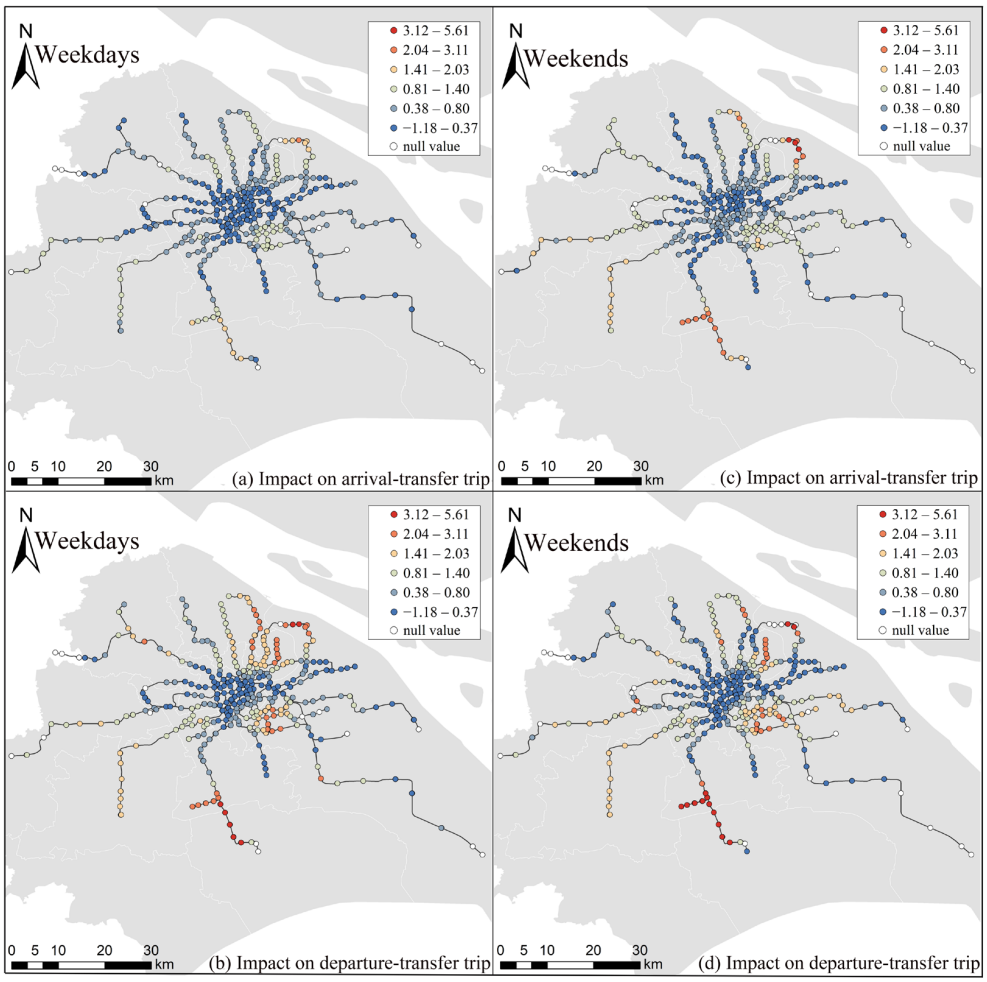


Figure 11. Spatial distributions of the average coefficients of hourly passenger flow.

Figure A2 shows the spatial distribution of the impact coefficient of transfer accessibility index on transfer trips. Figure A2a and Figure A2b, respectively, show the impact of transfer accessibility index on arrival-transfer trips and departure-transfer trips on weekdays. It can be found that in the city center, the impact coefficient of the transfer accessibility index on transfer trips is relatively high, while in suburban areas with a sparse distribution of subway stations, the impact coefficient of the transfer accessibility index on transfer trips is relatively low. There exist a few stations that have negative effects. The impact of the transfer accessibility index on arrival-transfer trips and departure-transfer trips on weekends is consistent with that on weekdays.

Figure A3 shows spatial distributions of the average coefficients of GDP. The result shows that the negative impact within the suburban subway station area is significant. The negative impact of GDP on transfer trips is mainly found in Putuo District, Songjiang District, Qingpu District, and Minhang District. In the Pudong New District, there is a slight positive or negative impact.

6. Discussion

The first-and-last mile problem plays a crucial role in people's daily travel. Undoubtedly, DBS significantly enhances the convenience for travelers in connecting with other travel modes. Traditional studies have focused on the relationship between the number of integrated trips and impact factors, like built environment and population density [7,47]; in this paper, we consider more impact factors, including built environment, population density, GDP, road density, metro passenger flow. Furthermore, we adopted two other factors to enrich our study, which are entropy of land use and transfer accessibility index. The existing research seldom studies the dynamic characteristics and the relationship between integrated trips and impact factors. Therefore, this paper studied the dynamic characteristics of integrated trips and proposed a GTWR model to study the correlations with impact factors based on a weekly data. Our findings show that the distributions of the number of passengers for the metro, DBS, and integrated trips are similar with each other, exhibiting two peaks on weekdays.

In this paper, the integrated DBS and metro trips are divided into arrival-transfer trips and departure-transfer trips. We studied the temporal and spatial features of the coefficient of metro passenger flow, the entropy of land use, the transfer accessibility index, and GDP based on the GTWR model. The results show that the effects of metro passenger flow on both two kinds of integrated trips are weaker during peak hours than in off-peak hours. The reason may be that passengers dislike to use bike-sharing to connect to the metro in peak hours due to the low speed of bikes and bad road conditions in some areas. The effects of hourly passenger flow on both arrival-transfer trips and departure-transfer trips in the central area are small, while they are stronger in the suburbs. The reason is that there are more traffic facilities in the central area of the city than in the suburbs, and travelers can choose other travel modes to connect metro stations [9].

The limitations of this study are as follows: It is difficult to identify the integrated trips from all DBS trips accurately. This paper adopted the widely used buffer zone with a 100 m radius and then matched the metro operation time. However, there are still limitations in this study in terms of identifying the integrated trips more accurately due to the lack of a trip chain of travelers. In terms of the buffer zone, how to set the suitable radius value needs further study. This study only considered the DBS and metro systems and did not involve other travel modes. In reality, there exist cooperation and competition among multimodal transportation, which may influence the integrated use of DBS and the metro. For example, the ground-level bus is the dominating feeder mode for metro systems [31]. In future study, more travel modes, such as taxis, busses, and private vehicles, will be considered in order to attain a comprehensive understanding of human travel behaviors in a city.

This study could provide suggestions for bike-sharing operators, bike-sharing users, and city managers in the decision-making process. The results encourage users to use bike-sharing to transfer to the metro before peak hours due to the good road conditions. For the bike-sharing operators, it is suggested that they should deploy more bike-sharing near the metro stations in morning peak hours because it is found that the number of departure-transfer trips are extremely high during the morning peaks. The reason is that more users used bike-sharing to get to their workplace after using the metro in the morning. Moreover, operators should provide more bikes in the suburbs because the demand for DBS–metro is larger due to the lack of travel facilities. In addition, the government should try their best to solve the parking problems near metro stations, i.e., that there are not enough parking places near most metro stations.

7. Conclusions

This study proposed a framework within which to investigate the travel mobility patterns of integrated DBS and metro use. First, a two-level process was built to identify integrated trips. Then, the spatiotemporal characteristics of the integrated trips, including travel distance, travel time, transfer accessibility index, and entropy of land use, were

detected based on multisource data. Finally, a GTWR model was developed to examine the correlations between the number of integrated trips and impact factors. The main findings are summarized as follows:

- The integrated trips account for 16.8% of total DBS trips based on the two-level identification method. A total of 59.6% of integrated trips are departure-transfer trips, and the rest are arrival trips. The travel distances of integrated trips are concentrated between 0 km and 2 km. Moreover, the distributions of the number of integrated trips per hour, including departure-transfer trips and arrival-transfer trips, are similar with DBS and the metro. In the spatial dimension, the integrated trips are concentrated in the central area of the city, while there is a small number of integrated trips in the suburbs.
- On the other hand, the transfer accessibility index and entropy of land use are analyzed. The results show that the transfer accessibility index in the central areas is much better than that in the suburbs. Moreover, it is observed that the transfer accessibility index values of both arrival-transfer trips and departure-transfer trips are larger on weekdays than on weekends. The entropy of land use in most buffer zones of metro stations has a large value, which means that the distributions of land type are more even.
- In terms of impact factors, it is found that GDP, government count, and restaurant count are negatively correlated with the number of integrated trips. In addition, we find that house price, entropy of land use, transfer accessibility index, and metro passenger flow show positive relationships with the number of integrated trips.
- The results show that the GTWR model outperforms the OLS model and the GWR model. Taking the impact factor of metro passenger flow as an example, we show the temporal and spatial distributions of the average coefficients of hourly passenger flow. The results show that the effects of metro passenger flow on both two kinds of integrated trips are weaker during peak hours than in off-peak hours. The effects of hourly metro passenger flow on both arrival-transfer trips and departure-transfer trips in central area are small, while they are stronger in the suburbs.

Author Contributions: Conceptualization, Hui Zhang; methodology, Yu Cui and Yanjun Liu; software, Yu Cui and Jianmin Jia; data curation, Hui Zhang, Yu Cui and Baiying Shi; writing—original draft preparation, Hui Zhang; writing—review and editing, Xiaohua Yu. All authors have read and agreed to the published version of the manuscript.

Funding: This work is supported by Youth Innovation Team Science and technology support project in Colleges and Universities of Shandong Province (2021KJ058, 2022KJ203), Shandong Provincial Natural Science Foundation (ZR2021MG032), Graduate Education Quality Improvement Plan program of Shandong Jianzhu University (YZKC202115).

Data Availability Statement: The data are not available due to privacy restrictions.

Conflicts of Interest: The authors declare no conflicts of interest.

Appendix A

Table A1. VIF values of selected explanatory variables of the OLS model for arrival-transfer trip.

Variables	Weekday			Weekend		
	Coef	*p*-Value	VIF	Coef	*p*-Value	VIF
Explanatory variables of socioeconomic						
GDP	−0.021	0.000	1.150	−0.034	0.000	1.152
House price	0.039	0.000	2.473	0.048	0.000	2.452
Population density	0.026	0.003	2.360	0.028	0.034	2.428
Explanatory variables of land use						
Hotel count	0.143	0.000	7.904	0.144	0.000	8.350

Table A1. *Cont.*

Variables	Weekday			Weekend		
Government count	−0.146	0.000	9.283	−0.243	0.000	9.866
Business count	/	/	/	/	/	/
Science and education culture count	/	/	/	0.150	0.000	4.016
Hospital count	0.050	0.000	5.363	0.089	0.000	5.451
Bus stop count	/	/	/	/	/	/
Restaurant count	−0.074	0.000	9.117	−0.089	0.004	9.512
Shopping mall count	/	/	/	/	/	/
Road density	/	/	/	/	/	/
Entropy of land use	0.023	0.004	1.920	0.043	0.000	1.915
Explanatory variables of metro						
Number of metro station	0.024	0.001	2.490	0.030	0.003	2.460
Hourly inbound passenger flow	0.413	0.000	1.142	0.287	0.000	1.172
Transfer accessibility index	0.260	0.000	1.050	0.140	0.000	1.014

Note: The sign "/" means explanatory variables with *p*-value lager than 0.05.

Table A2. VIF values of explanatory variables of the OLS model for departure-transfer trip.

Variables	Weekday			Weekend		
	Coef	*p*-Value	VIF	Coef	*p*-Value	VIF
Explanatory variables of socioeconomic						
GDP	−0.017	0.000	1.148	−0.037	0.000	1.153
House price	0.048	0.000	2.502	0.082	0.000	2.475
Population density	0.032	0.002	2.356	0.039	0.012	2.393
Explanatory variables of land use						
Hotel count	0.140	0.000	7.960	0.166	0.000	8.081
Government count	−0.160	0.000	9.334	−0.325	0.000	9.662
Business count	0.068	0.000	4.525	/	/	/
Science and education culture count	/	/	/	/	/	/
Hospital count	0.055	0.001	5.387	0.134	0.000	5.501
Bus stop count	0.026	0.024	3.512	0.045	0.009	3.558
Restaurant count	−0.086	0.001	9.155	−0.105	0.004	9.280
Shopping mall count	/	/	/	/	/	/
Road density	/	/	/	/	/	/
Entropy of land use	0.022	0.018	1.927	0.051	0.000	1.908
Explanatory variables of metro						
Number of metro station	/	/	/	/	/	/
Hourly outbound passenger flow	0.413	0.000	1.180	0.194	0.000	1.198
Transfer accessibility index	0.252	0.000	1.130	0.474	0.000	1.026

Note: The sign "/" means explanatory variables with *p*-value lager than 0.05.

Table A3. Moran's I test result for explanatory variables.

Variables	Moran's I	Z-Score	*p*-Value
Explanatory variables of socioeconomic			
GDP	0.666	22.794	0.000
House price	0.912	72.173	0.000
Population density	/	/	/
Explanatory variables of land use			
Hotel count	0.242	8.501	0.000
Government count	0.092	3.290	0.001
Business count	0.198	6.948	0.000
Science and education culture count	0.061	2.316	0.021
Hospital count	0.060	2.177	0.029
Bus stop count	/	/	/

Table A3. *Cont.*

Variables	Moran's I	Z-Score	*p*-Value
Restaurant count	0.077	2.756	0.006
Entropy of land use	0.067	2.383	0.017
Explanatory variables of metro			
Number of metro station	0.774	61.276	0.000
Hourly inbound passenger flow on weekdays	0.370	81.221	0.000
Hourly outbound passenger flow on weekdays	0.326	74.306	0.000
Hourly inbound passenger flow on weekends	0.660	134.261	0.000
Hourly outbound passenger flow on weekends	0.680	143.525	0.000
Hourly accessibility of arrival-transfer trips of each metro stations on weekdays	0.063	13.889	0.000
Hourly accessibility of departure-transfer trips of time at each metro stations on weekdays	0.183	41.488	0.000
Hourly accessibility of arrival-transfer trips of time at each metro stations on weekends	0.032	6.463	0.000
Hourly accessibility of departure-transfer trips of time at each metro stations on weekends	0.096	20.390	0.000

Note: The sign "/" means explanatory variables with *p*-value lager than 0.05.

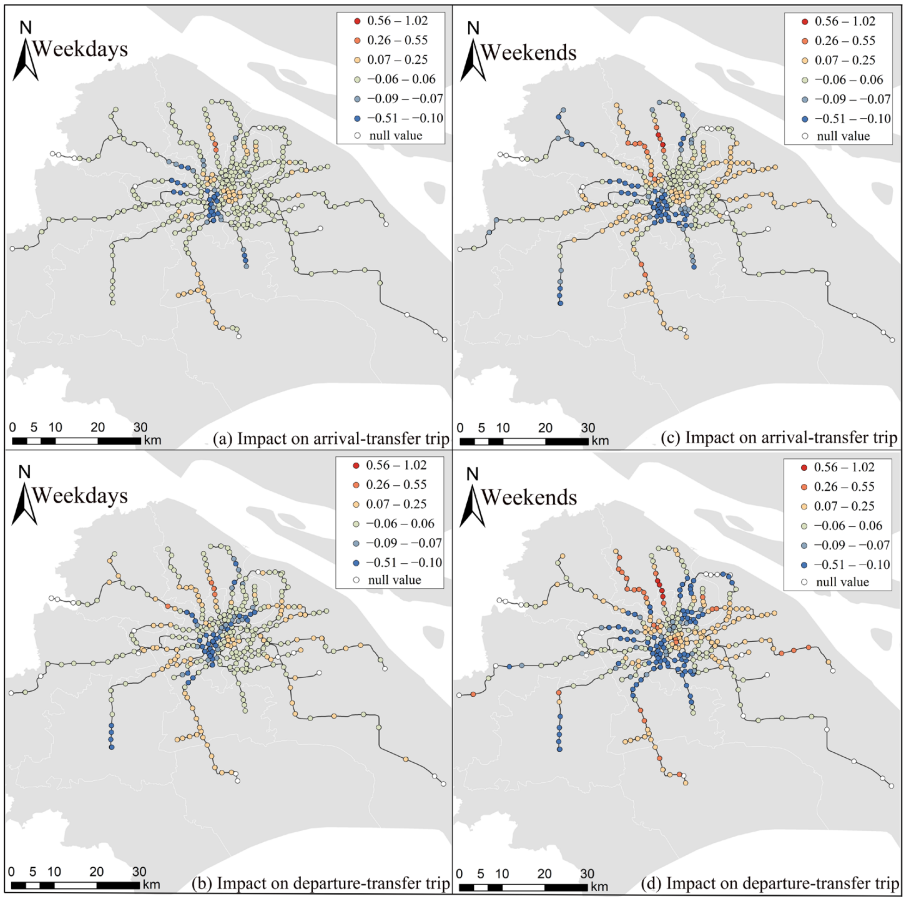


Figure A1. Spatial distributions of the average coefficients of the entropy of land use.

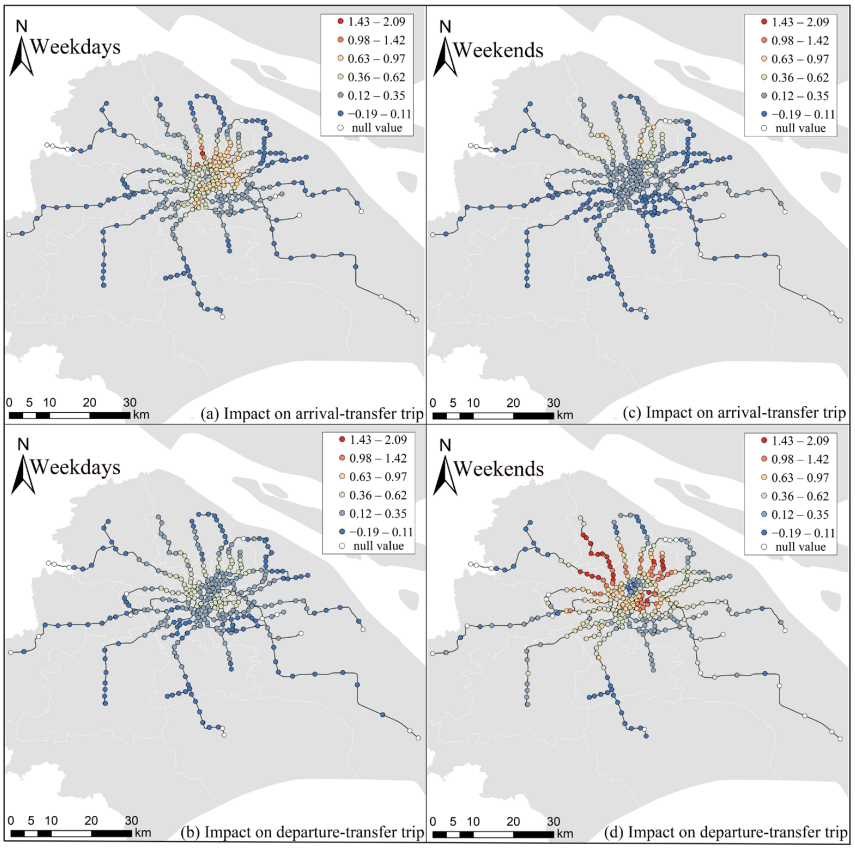


Figure A2. Spatial distributions of the average coefficients of the transfer accessibility index.

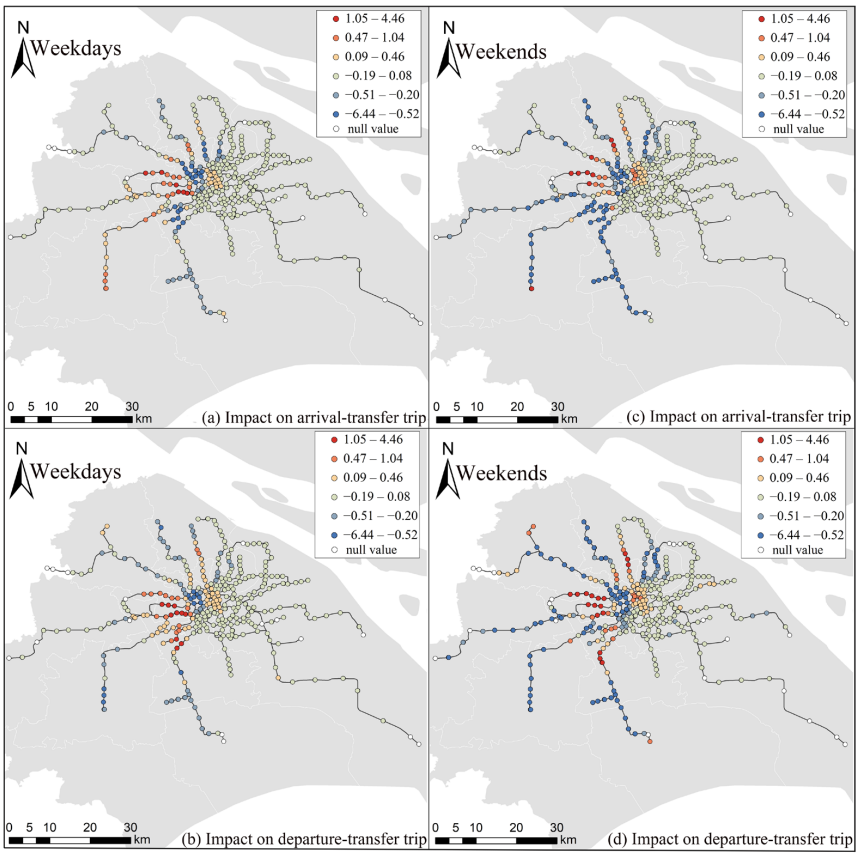


Figure A3. Spatial distributions of the average coefficients of GDP.

References

1. Chen, Z.W.; Guo, Y.J.; Stuart, A.L.; Zhang, Y.; Li, X.P. Exploring the equity performance of bike-sharing systems with disaggregated data: A story of southern Tampa. *Transp. Res. A* **2019**, *130*, 529–545. [CrossRef]
2. Wu, C.L.; Kim, I. Analyzing the structural properties of bike-sharing networks: Evidence from the United States, Canada, and China. *Transp. Res. A* **2020**, *140*, 52–71. [CrossRef]
3. Giuffrida, N.; Pilla, F.; Carroll, P. The social sustainability of cycling: Assessing equity in the accessibility of bike-sharing services. *J. Transp. Geogr.* **2023**, *106*, 103490. [CrossRef]
4. Jia, J.M.; Liu, C.S.; Wang, X.H.; Zhang, H.; Xiao, Y. Understanding bike-sharing mobility in response to the COVID-19 pandemic. *Cities* **2023**, *142*, 104554. [CrossRef]
5. Zhang, X.X.; Zhang, Q.N.; Sun, T.T.; Zou, Y.C.; Chen, H.W. Evaluation of urban public transport priority performance based on the improved TOPSIS method: A case study of Wuhan. *Sustain. Cities Soc.* **2018**, *43*, 357–365. [CrossRef]
6. Fan, Y.C.; Zheng, S.Q. Dockless bike sharing alleviates road congestion by complementing subway travel: Evidence from Beijing. *Cities* **2020**, *107*, 102895. [CrossRef]
7. Li, W.X.; Chen, S.W.; Dong, J.S.; Wu, J.X. Exploring the spatial variations of transfer distance between dockless bike-sharing systems and metro. *J. Transp. Geogr.* **2021**, *92*, 103032. [CrossRef]
8. Wu, H.; Wang, Y.H.; Sun, Y.Q.; Yin, D.D.; Li, Z.X.; Luo, X.Y. Identification and spatiotemporal analysis of bikesharing-metro integration cycling. *ISPRS Int. J. Geo-Inf.* **2023**, *12*, 166. [CrossRef]
9. Guo, Y.Y.; He, S.Y. Built environment effects on the integration of dockless bike-sharing and the metro. *Transp. Res. D* **2020**, *83*, 102335. [CrossRef]
10. Liu, S.Y.; Zhou, C.J.; Rong, J.; Bian, Y.; Wang, Y. Concordance between regional functions and mobility features using bike-sharing and land use data near metro stations. *Sustain. Cities Soc.* **2022**, *84*, 104010. [CrossRef]
11. Kim, J.; Lee, S. Determining factors affecting public bike ridership and its spatial change before and after COVID-19. *Travel Behav. Soc.* **2023**, *31*, 24–36. [CrossRef] [PubMed]
12. Li, X.F.; Du, M.Y.; Yang, J.Z. Factors influencing the access duration of free-floating bike sharing as a feeder to the metro in Shenzhen. *J. Clean. Prod.* **2020**, *277*, 123273. [CrossRef]
13. Yen, B.T.H.; Mulley, C.; Yeh, C.J. How public shared bike can assist first and last mile accessibility: A case study of the MRT system in Taipei city, Taiwan. *J. Transp. Geogr.* **2023**, *108*, 103569. [CrossRef]
14. Meng, F.Y.; Zheng, L.L.; Ding, T.Q.; Wang, Z.R.; Zhang, Y.L.; Li, W.Q. Understanding dockless bike-sharing spatiotemporal travel patterns: Evidence from ten cities in China. *Comput. Environ. Urban* **2023**, *104*, 102006. [CrossRef]
15. Xu, X.J.; Wang, J.; Poslad, S.; Rui, X.P.; Zhang, G.Y.; Fan, Y.L. Exploring intra-urban human mobility and daily activity patterns from the lens of dockless bike-sharing: A case study of Beijing, China. *Int. J. Appl. Earth Obs. Geoinf.* **2023**, *122*, 103442. [CrossRef]
16. Qiu, W.S.; Chang, H.C. The interplay between dockless bikeshare and bus for small-size cities in the US: A case study of Ithaca. *J. Transp. Geogr.* **2021**, *96*, 103175. [CrossRef]
17. Martin, R.; Xu, Y.L. Is tech-enhanced bikeshare a substitute or complement for public transit? *Transp. Res. A* **2022**, *155*, 63–78. [CrossRef]
18. Zhao, D.; Ong, G.P.; Wang, W.; Hu, X.J. Effect of built environment on shared bicycle reallocation: A case study on Nanjing, China. *Transp. Res. A* **2019**, *128*, 73–88. [CrossRef]
19. Zheng, L.L.; Meng, F.Y.; Ding, T.Q.; Yang, Q.F.; Xie, Z.F.; Jiang, Z.T. The effect of traffic status on dockless bicycle-sharing: Evidence from Shanghai, China. *J. Clean. Prod.* **2022**, *381*, 135207. [CrossRef]
20. Mohiuddin, H.; Fitch-Polse, D.T.; Handy, S.L. Does bike-share enhance transport equity? Evidence from the Sacramento, California region. *J. Transp. Geogr.* **2023**, *109*, 103588. [CrossRef]
21. Shi, X.Y.; Zhao, J.J.; He, J.M.; Xu, H.T. Exploring year-to-year spatiotemporal changes in cycling patterns for bike-sharing system in the pre-, during and post-pandemic periods. *Sustain. Cities Soc.* **2023**, *98*, 104814. [CrossRef]
22. Liu, S.Y.; Zhang, X.D.; Zhou, C.J.; Rong, J.; Bian, Y. Temporal heterogeneous effects of land-use on dockless bike-sharing usage under transit-oriented development context: The case of Beijing. *J. Clean. Prod.* **2022**, *380*, 134917. [CrossRef]
23. Zhao, P.J.; Li, S.X. Bicycle-metro integration in a growing city: The determinants of cycling as a transfer mode in metro station areas in Beijing. *Transp. Res. A* **2017**, *99*, 46–60. [CrossRef]
24. Liu, L.M.; Kong, H.; Liu, T.L.; Ma, X.L. Mode choice between bus and bike-sharing for the last-mile connection to urban rail transit. *J. Transp. Eng. A* **2022**, *148*, 04022017. [CrossRef]
25. Ji, Y.J.; Fan, Y.L.; Ermagun, A.; Cao, X.N.; Wang, W.; Das, K. Public bicycle as a feeder mode to rail transit in China: The role of gender, age, income, trip purpose, and bicycle theft experience. *Int. J. Sustain. Transp.* **2017**, *11*, 308–317. [CrossRef]
26. Du, Y.C.; Deng, F.W.; Liao, F.X. A model framework for discovering the spatio-temporal usage patterns of public free-floating bike-sharing system. *Transp. Res. C* **2019**, *103*, 39–55. [CrossRef]
27. Lin, D.; Zhang, Y.P.; Zhu, R.X.; Meng, L.Q. The analysis of catchment areas of metro stations using trajectory data generated by dockless shared bikes. *Sustain. Cities Soc.* **2019**, *49*, 101598. [CrossRef]
28. Xing, Y.Y.; Wang, K.; Lu, J.J. Exploring travel patterns and trip purposes of dockless bike-sharing by analyzing massive bike-sharing data in Shanghai, China. *J. Transp. Geogr.* **2020**, *87*, 102787. [CrossRef]
29. Yu, S.B.; Liu, G.H.; Yin, C.R. Understanding spatio-temporal travel demand of free-floating bike sharing connecting with metro stations. *Sustain. Cities Soc.* **2021**, *74*, 103162. [CrossRef]

30. Liu, S.M.; Zhang, F.; Ji, Y.J.; Ma, X.W.; Liu, Y.; Li, S.; Zhou, X.Z. Understanding spatial-temporal travel demand of private and shared e-bikes as a feeder mode of metro stations. *J. Clean. Prod.* **2023**, *398*, 136602. [CrossRef]
31. Shi, Y.J. Identifying the spatiotemporal metro-to-bus transfer deserts in Shanghai, China. *J. Urban. Plan. Dev.* **2023**, *149*, 04023013. [CrossRef]
32. Zhang, X.H.; Shen, Y.; Zhao, J.H. The mobility pattern of dockless bike sharing: A four-month study in Singapore. *Transp. Res. D* **2021**, *98*, 102961. [CrossRef]
33. Zhu, R.; Zhang, X.H.; Kondor, D.; Santi, P.; Ratti, C. Understanding spatio-temporal heterogeneity of bike-sharing and scooter-sharing mobility. *Comput. Environ. Urban* **2020**, *81*, 101483. [CrossRef]
34. Li, Y.X.; Dai, Z.X.; Zhu, L.N.; Liu, X.L. Analysis of spatial and temporal characteristics of citizens' mobility based on E-bike GPS trajectory data in Tengzhou city, China. *Sustainability* **2019**, *11*, 5003. [CrossRef]
35. Zheng, Z.G.; Chen, Y.F.; Zhu, D.B.; Sun, H.J.; Wu, J.J.; Pan, X.; Li, D.Q. Extreme unbalanced mobility network in bike sharing system. *Phys. A* **2021**, *563*, 125444. [CrossRef]
36. Yang, Y.X.; Heppenstall, A.; Turner, A.; Comber, A. A spatiotemporal and graph-based analysis of dockless bike sharing patterns to understand urban flows over the last mile. *Comput. Environ. Urban* **2019**, *77*, 101361. [CrossRef]
37. Tian, Z.H.; Zhou, J.; Wang, M.G. Dynamic evolution of demand fluctuation in bike-sharing systems for green travel. *J. Clean. Prod.* **2019**, *231*, 1364–1374. [CrossRef]
38. Zhang, H.; Zhuge, C.X.; Jia, J.M.; Shi, B.Y.; Wang, W. Green travel mobility of dockless bike-sharing based on trip data in big cities: A spatial network analysis. *J. Clean. Prod.* **2021**, *313*, 127930. [CrossRef]
39. Yang, Y.X.; Heppenstall, A.; Turner, A.; Comber, A. Using graph structural information about flows to enhance short-term demand prediction in bike-sharing systems. *Comput. Environ. Urban* **2020**, *83*, 101521. [CrossRef]
40. Xiao, G.N.; Wang, R.N.; Zhang, C.Q.; Ni, A.N. Demand prediction for a public bike sharing program based on spatio-temporal graph convolutional networks. *Multimed. Tools Appl.* **2021**, *80*, 22907–22925. [CrossRef]
41. Li, X.Y.; Xu, Y.; Zhang, X.H.; Shi, W.Z.; Yue, Y.; Li, Q.Q. Improving short-term bike sharing demand forecast through an irregular convolutional neural network. *Transp. Res. C* **2023**, *147*, 103984. [CrossRef]
42. Dastjerdi, A.M.; Morency, C. Bike-sharing demand prediction at community level under COVID-19 using deep learning. *Sensors* **2022**, *22*, 1060. [CrossRef] [PubMed]
43. Hu, S.H.; Xiong, C.F.; Liu, Z.Q.; Zhang, L. Examining spatiotemporal changing patterns of bike-sharing usage during COVID-19 pandemic. *J. Transp. Geogr.* **2021**, *91*, 102997. [CrossRef]
44. Li, A.Y.; Zhao, P.X.; Haitao, H.; Mansourian, A.; Axhausen, K.W. How did micro-mobility change in response to COVID-19 pandemic? A case study based on spatial-temporal-semantic analytics. *Comput. Environ. Urban* **2021**, *90*, 101703. [CrossRef] [PubMed]
45. Li, H.W.; Xing, Y.Y.; Zhang, W.B.; Zhang, X.L. Investigating the impact of weather conditions and land use on dockless bike-share trips in Shanghai, China. *J. Urban. Plan. Dev.* **2021**, *147*, 05021031. [CrossRef]
46. Wu, C.L.; Kim, I.; Chung, H. The effects of built environment spatial variation on bike-sharing usage: A case study of Suzhou, China. *Cities* **2021**, *110*, 103063. [CrossRef]
47. Zhou, X.; Dong, Q.H.; Huang, Z.; Yin, G.M.; Zhou, G.Q.; Liu, Y. The spatially varying effects of built environment characteristics on the integrated usage of dockless bike-sharing and public transport. *Sustain. Cities Soc.* **2023**, *89*, 104348. [CrossRef]
48. Chai, X.W.; Guo, X.; Xiao, J.H.; Jiang, J. Analysis of spatiotemporal mobility of shared-bike usage during COVID-19 pandemic in Beijing. *Trans. GIS* **2021**, *25*, 2866–2887. [CrossRef] [PubMed]
49. Kwon, K.; Akar, G. What determines modal substitution between bike-sharing and public transit? Evidence from Columbus, Ohio during the COVID-19 pandemic. *Int. J. Sustain. Transp.* **2023**, *17*, 1087–1096. [CrossRef]
50. Kim, M.; Cho, G.H. Examining the causal relationship between bike-share and public transit in response to the COVID-19 pandemic. *Cities* **2022**, *131*, 104024. [CrossRef] [PubMed]
51. Li, A.Y.; Zhao, P.X.; Huang, Y.Z.; Gao, K.; Axhausen, K.W. An empirical analysis of dockless bike-sharing utilization and its explanatory factors: Case study from Shanghai, China. *J. Transp. Geogr.* **2020**, *88*, 102828. [CrossRef]
52. Bi, H.; Li, A.Y.; Hua, M.Z.; Zhu, H.; Ye, Z.R. Examining the varying influences of built environment on bike-sharing commuting: Empirical evidence from Shanghai. *Transp. Policy* **2022**, *129*, 51–65. [CrossRef]
53. Murray, A.T. Strategic analysis of transport coverage. *Socio-Econ. Plan. Sci.* **2001**, *35*, 175–188. [CrossRef]
54. Currie, G. Quantifying spatial gaps in public transport supply based on social needs. *J. Transp. Geogr.* **2010**, *18*, 31–41. [CrossRef]
55. Guzman, L.A.; Oviedo, D.; Rivera, C. Assessing equity in transport accessibility to work and study: The Bogota region. *J. Transp. Geogr.* **2017**, *58*, 236–246. [CrossRef]
56. Tahmasbi, B.; Haghshenas, H. Public transport accessibility measure based on weighted door to door travel time. *Comput. Environ. Urban* **2019**, *76*, 163–177. [CrossRef]
57. Xu, W.T.; Yang, L.C. Evaluating the urban land use plan with transit accessibility. *Sustain. Cities Soc.* **2019**, *45*, 474–485. [CrossRef]
58. Grava, S. Urban transportation systems: Choice for communities. *IEEE Trans. Autom. Control* **2003**, *55*, 737–743.
59. Ma, X.L.; Zhang, X.; Li, X.; Wang, X.J.; Zhao, X. Impacts of free-floating bikesharing system on public transit ridership. *Transp. Res. D* **2019**, *76*, 100–110. [CrossRef]
60. Li, X.; Liu, Z.; Ma, X. Measuring access and egress distance and catchment area of multiple feeding modes for metro transferring using survey data. *Sustainability* **2022**, *14*, 2841. [CrossRef]

61. Chen, Z.Y.; van Lierop, D.; Ettema, D. Perceived accessibility: How access to dockless bike-sharing impacts activity participation. *Travel Behav. Soc.* **2022**, *27*, 128–138. [CrossRef]
62. Yang, M.; Zhao, J.Y.; Wang, W.; Liu, Z.Y.; Li, Z.B. Metro commuters' satisfaction in multi-type access and egress transferring groups. *Transp. Res. D* **2015**, *34*, 179–194. [CrossRef]
63. Paydar, M.; Fard, A.K.; Khaghani, M.M. Walking toward metro stations: The contribution of distance, attitudes, and perceived built environment. *Sustainability* **2020**, *12*, 10291. [CrossRef]
64. Zhao, D.; Wang, W.; Li, C.Y.; Ji, Y.J.; Hu, X.J.; Wang, W.F. Recognizing metro-bus transfers from smart card data. *Transp. Plan. Technol.* **2019**, *42*, 70–83. [CrossRef]
65. Shao, H.Y.; Jin, C.; Xu, J.; Zhong, Y.X.; Qiu, M.X. Identifying metro station types based on transfer purposes: An application of bike-sharing data in Xiamen, China. *Can. Geogr.-Geogr. Can.* **2023**, *67*, 550–563. [CrossRef]
66. Zhong, J.M.; He, Z.C.; Xie, J.M. Revealing the travel community in the integrated system of free-floating bike and metro. *Sustain. Cities Soc.* **2023**, *97*, 104760. [CrossRef]
67. Wu, X.Y.; Lu, Y.; Lin, Y.Y.; Yang, Y.Y. Measuring the destination accessibility of cycling transfer trips in metro station areas: A big data approach. *Int. J. Environ. Res. Public Health* **2019**, *16*, 2641. [CrossRef] [PubMed]
68. Liu, X.H.; Fan, J.; Li, Y.; Shao, X.; Lai, Z.L. Analysis of integrated uses of dockless bike sharing and ridesourcing with metro: A case study of Shanghai, China. *Sustain. Cities Soc.* **2022**, *82*, 103918. [CrossRef]
69. Housing Price Report. Available online: https://shanghai.anjuke.com/?from=AJKWebCity (accessed on 1 August 2018).
70. Tu, W.; Cao, R.; Yue, Y.; Zhou, B.D.; Li, Q.P.; Li, Q.Q. Spatial variations in urban public ridership derived from GPS trajectories and smart card data. *J. Transp. Geogr.* **2018**, *69*, 45–57. [CrossRef]
71. Romos-Santiago, L.E.; Brown, J. A comparative assessment of the factors associated with station-level streetcar versus light rail transit ridership in the United States. *Urban Stud.* **2016**, *53*, 915–935. [CrossRef]
72. Yang, C.; Yu, C.C.; Dong, W.T.; Yuan, Q. Substitutes or complements? Examining effects of urban rail transit on bus ridership using longitudinal city-level data. *Transp. Res. A* **2023**, *174*, 103728. [CrossRef]
73. Chien, Y.M.C.; Carver, S.; Comber, A. Using geographically weighted models to explore how crowdsourced landscape perceptions relate to landscape physical characteristics. *Landsc. Urban Plan.* **2020**, *203*, 103904. [CrossRef]
74. Brunsdon, C.; Fotheringham, A.S.; Charlton, M.E. Geographically weighted regression: A method for exploring spatial nonstationarity. *Geogr. Anal.* **1996**, *28*, 281–298. [CrossRef]
75. Huang, B.; Wu, B.; Barry, M. Geographically and temporally weighted regression for modeling spatio-temporal variation in house prices. *Int. J. Geogr. Inf. Sci.* **2010**, *24*, 383–401. [CrossRef]
76. Ma, X.W.; Ji, Y.J.; Yuan, Y.F.; Van Oort, N.; Jin, Y.C.; Hoogendoorn, S. A comparison in travel patterns and determinants of user demand between docked and dockless bike-sharing systems using multi-sourced data. *Transp. Res. A* **2020**, *139*, 148–173. [CrossRef]
77. Huang, B.; Wang, J. GTWRv1_1_20_May2020.zip. Available online: https://www.researchgate.net/publication/339567248_GTWRv1_1_20_May2020zip (accessed on 24 April 2020).

Disclaimer/Publisher's Note: The statements, opinions and data contained in all publications are solely those of the individual author(s) and contributor(s) and not of MDPI and/or the editor(s). MDPI and/or the editor(s) disclaim responsibility for any injury to people or property resulting from any ideas, methods, instructions or products referred to in the content.